The Journal of Experimental Biology 208, 4213-4222
Published by The Company of Biologists 2005
doi:10.1242/jeb.01896

Response properties of electrosensory afferent fibers and secondary brain stem neurons in the paddlefish

Michael H. Hofmann[1,*], Boris Chagnaud[1] and Lon A. Wilkens[2]

[1]*University of Bonn, Institute of Zoology, Poppelsdorfer Schloss, 53115 Bonn, Germany* and [2]*Center for Neurodynamics, Department of Biology, University of Missouri-St Louis, MO 63121, USA*

*Author for correspondence (e-mail: mhofmann@uni-bonn.de)

Accepted 22 September 2005

Summary

The passive electrosense is used by many aquatic animals to detect weak electric fields from other animals or from geoelectric sources. In contrast to the active electrosense, 'passive' means that there are no electric organs, and only external fields are measured. Electroreceptors are distributed in the skin, but are different from other skin senses because they can detect and localize sources a considerable distance away. Distant sources, however, stimulate a large number of receptors at the same time and central circuits have to compute the exact location of the source from this distributed information. In order to gain insights into the algorithms involved, we compared the response properties of units in the dorsal octavolateral nucleus (DON) with primary afferent fibers in the paddlefish. The following parameters were tested: spontaneous activity, sensitivity, frequency tuning, receptive field size, movement sensitivity, and topography within the DON. Although there are some differences in spontaneous activity and receptive field size, there are no major differences between primary afferents and DON units that could reveal any substantial amount of spatial information processing. In particular the lack of any topographic order whithin the DON renders a lateral interaction between neighboring receptive fields unlikely.

Key words: passive electroreception, paddlefish, *Polyodon spathula*, dorsal octavolateral nucleus, topography.

Introduction

Passive electrosensory animals can detect weak electric fields created by other animals and use this information to detect prey or avoid predators (Wilkens and Hofmann, 2004). Electric fields are also generated by geochemical phenomena or by induction of objects moving through the earth's magnetic field (Kalmijn, 1984). The passive electrosense is present in many aquatic animals, including lampreys (Bodznick and Northcutt, 1982), sharks and rays (Kalmijn, 1966; Bodznick and Boord, 1986; Tricas and New, 1998), sturgeons (Northcutt, 1986) and paddlefish (Gurgens et al., 2000; Wilkens et al., 2001), some groups of advanced bony fishes (Finger et al., 1986; Fortune and Rose, 1997), lungfishes (Roth, 1973), many amphibians (Fritzsch and Münz, 1986; Roth and Schlegel, 1988), and even in mammals, i.e. platypus and echidna (Gregory et al., 1987; Pettigrew, 1999). Electroreceptors measure the difference in field strength between an external pore and an internal reference. The pores are distributed over the head and gill covers in non-teleosts, with additional pores on the trunk in teleosts (advanced bony fishes).

In 'proximity mode', electroreceptors probably work like the more familiar somatosensory system in that they 'feel' the presence of an object by its electric field, and the location of the object is determined by which receptors are stimulated. However, electroreception is different from the somatosensory system in that it can also detect objects a considerable distance away (e.g. Wilkens et al., 2001). In this 'distance mode', a single source stimulates a large number of receptors simultaneously and the exact source location has to be computed centrally. This is comparable to an array of photoreceptors, but without an image-forming lens.

At present, it is unknown how the brain can compute electrosensory information in this 'distance mode'. To begin to address this question, we investigated signal processing in the first relay center of the paddlefish, the dorsal octavolateral nucleus (DON), by comparing the response properties of the second order neurons in the DON with those of the primary afferent fibers, which carry the information from peripheral receptors to the brain. Differences in the following parameters were tested: receptive field shape (lateral inhibition, contrast enhancement), movement detection, topography within the DON, sensitivity and frequency tuning.

Materials and methods

Animals

Twenty-two paddlefish (*Polyodon spathula* Walbaum 1792) measuring 20–30 cm total length were used for this investigation. They were obtained from the Blind Pony Fish Hatchery, Missouri Department of Conservation and kept in a

round tank, approximately 2000 l, bio-filtered and oxygenated. The tank contained dechlorinated tapwater raised to a salinity of 2‰ by the addition of stock salt. Before surgery, the animals were anesthetized with MS-222 (1:10000 v/v) and the brain exposed. The animals were then placed in a recording tank, immobilized with 10 μl Tubocurarine (Apothecon) and the gills were irrigated with freshwater through the mouth.

Stimulation

Electrical stimuli were either large quasi-uniform fields or local dipole sources, which were moved along the rostro-caudal axis parallel to the rostrum of the fish. Quasi-uniform electric fields were produced by two silver wires, one 10 cm in front of the animal and one 5 cm behind it. The wires were connected to a constant current source (A 395 linear stimulus isolator, WPI, Sarasota, FL, USA) driven by a sound card of a PC. The sound card was modified to allow stimulus waveforms down to true DC. Custom-made software drove the sound card with 16-bit resolution and 10 kHz sampling rate. Uniform fields were used as search stimuli (25 $\mu V\ cm^{-1}$, modulated at 5 Hz).

The moving dipole fields were produced by three silver wires placed 4 mm apart. Two of them were arranged parallel to the rostro-caudal axis of the rostrum, and used for dipolar stimulation. Here the term dipolar refers to the fact that, in this configuration, a given receptor was first under the influence of the leading electrode and, when the center of the dipole has passed over the receptor, the response was dominated by the trailing electrode. In a monopolar configuration, a third electrode positioned 4 mm laterally to the first electrode was used as the second pole. In this configuration, where the electrodes were oriented perpendicular to the movement direction, the first electrode was always proximal to the fish.

The electrodes were translated by a linear stepping motor (LinMot, Sulzer Electronics, Zürich, Switzerland) parallel to the rostro-caudal axis at a distance 2 cm from the edge of the rostrum. In order to scan the receptive field, we delivered a continuous 2 Hz sinusoidal stimulus while moving the electrodes slowly (0.5 $cm\ s^{-1}$) from rostral to caudal and, after a brief pause, back to rostral. To test for movement detection, we applied a DC field and moved it at a speed of 5 $cm\ s^{-1}$, approximating the normal swimming speed of the paddlefish. Further processing of the data is described below.

Calibration

Calibration of the stimuli was done by measuring the electric field in the experimental setup with two silver wires placed 2 cm apart parallel to the electric field. The signal was amplified with a differential DC amplifier and viewed on an oscilloscope. Due to possible polarization effects, noise and DC offsets, only large amplitude fields in the range of 1000–5000 $\mu V\ cm^{-1}$ could be picked up. Even with these large amplitudes, DC fields were stable over long periods and sine waves and other wave forms showed no distortion due to polarization of the stimulation electrodes.

To test the linearity of the electric fields down to the low amplitudes used during the recordings (i.e. <50 $\mu V\ cm^{-1}$), one of the calibration electrodes was vibrated parallel to the electric field with an amplitude of 4 cm at 5 or 10 Hz. The modulated signal was amplified, digitized, and band-pass filtered at the modulation frequency and the peak-to-peak amplitude determined. Since only the modulation due to the vibration was measured, any DC offset was eliminated. With this method, we could assure the linearity of the stimulus down to electric fields of <10 $\mu V\ cm^{-1}$.

The stimulus intensities used in our experiments were tested for their behavioral relevance in freely moving paddlefish. Local DC dipole fields with an intensity up to ten times stronger than the one used in the electrophysiological recordings (<50 $\mu V\ cm^{-1}$) elicited prey catching behavior. Only much stronger or larger dimension electric fields resulted in avoidance behavior (>100 μV and dipole size >5 cm). Thus, the stimuli used in our electrophysiological studies were within an intensity range that elicited natural behaviors in the paddlefish.

Recording

Single unit activity was recorded in the hind brain dorsal octavolateral nucleus (DON) with tungsten electrodes (5–20 MΩ) and from primary afferent fibers in the lateral line ganglia with glass electrodes (>30 MΩ, filled with 3% lithium chloride). With tungsten electrodes we were able to record single units in the DON, but not in the lateral line nerve or ganglion. The signals were amplified by 1000 (AM Systems, model 1700, Carlsborg, WA, USA), filtered (notch, 300 Hz low pass, 5 kHz high pass), displayed on an oscilloscope (Tektronix, 2216, Richardson, TX, USA) and monitored on a loudspeaker. The amplified signals were fed through a window discriminator (121 Window Discriminator, WPI, Sarasote, FL, USA) and the TTL pulses were recorded on a computer with a commercial sound card at a sampling rate of 10 kHz. To ensure synchrony of the recordings with the stimulation, a trigger pulse was generated by the computer at the start of the stimulation. This pulse was recorded simultaneously with the spike data.

Data analysis

The data were further analyzed using IGOR 4 software (Wavemetrics, Lake Oswego, OR, USA). For every stimulus paradigm, the instantaneous firing rate was calculated. For stimulus durations of 1 s or less, the stimuli were repeated ten times and the firing rate averaged. Longer recordings were repeated five times, although very slow sine waves lasting more than 10 s were recorded only once. The spontaneous firing rates were recorded for 1 min.

Beside calculating the mean firing rate, the temporal structure of interspike intervals was analyzed by autocorrelation. Primary afferent fibers show a characteristic spike pattern that can be detected by autocorrelation analysis (Bahar et al., 2001). The mean interspike interval was

subtracted from each interval ($\Delta t_i = t_i - t$) and the autocorrelation $C(n)$ of the Δt_i calculated as:

$$C(n) = \frac{1}{N-n} \sum_{i=1}^{N-n} \Delta t_i \Delta t_{i+n} , \quad (1)$$

where N is the total number of intervals in the data set. For n=1, the function returns the correlation of each interval with the following one; n=2 returns the correlation of each interval with the after next one and so on. If the intervals were uncorrelated the return value would be zero. If the function results in a positive value the intervals are correlated and if it is a negative value they are anticorrelated, i.e. long intervals are followed by short ones and *vice versa*. For each spike train, we also shuffled the sequence of intervals such that the sequence of all intervals was randomized, thus destroying any temporal relationships between intervals. The autocorrelation of the shuffled data was used as baseline correlation and the correlation within the original spike train was calculated as the root mean square of the correlation divided by the root mean square of the correlation of the shuffled data. In order to detect only long-range autocorrelation, we used n values from 5 to 50, i.e. correlations of each interval with the next five intervals were ignored.

Data obtained during slow scanning of the receptive fields with the linear stepping motor and a 2 Hz AC field were converted into an instantaneous frequency plot (Fig. 1A), normalized, filtered around the stimulation frequency, and multiplied by the 2 Hz stimulus (Fig. 1B). This multiplication results in a signal whose amplitude reflects the response magnitude and whose polarity represents the phase. This kind of computation is referred to as the phase plot. Fig. 1 shows an example of a 2 Hz stimulation with local electrodes oriented perpendicular to the rostrum, and moved at a speed of 0.5 cm s^{-1} along the rostro-caudal axis of the rostrum. Fig. 1A shows the firing rate of a DON unit and Fig. 1B the corresponding phase plot. Whereas the original data (Fig. 1A) reveal only the response magnitude, Fig. 1B shows the phase relationship between the stimulus and the response in addition. The multiplication with the stimulus results in a signal with twice the frequency. The maximum response is reached when the electrodes are over the center of the receptive field. The phase as reflected by the sign indicates whether the unit responds with an increase of firing when the stimulus is positive or negative. The phase plot is therefore able to reveal, for example, lateral inhibition or center-surround organization, where the center of a receptive field is surrounded by an area where the polarity of the response is reversed.

Along with the receptive field, the location of the cell within the DON was determined by the following procedure. On a photograph of the exposed brain taken immediately after the surgery, the position of the electrode was marked according to measurements from the preparation. After the experiment, the head was fixed with 4% paraformaldehyde and the meninges removed to expose the brain surface. The DON was clearly visible as a crest on the hind brain and its outline was superimposed onto the photograph. The position of each DON unit was then calculated as percent of DON length and width, respectively.

Results

Recordings were made from primary afferent fibers (PA) in the lateral line nerves and from units in the dorsal octavolateral nucleus (DON). PA were recorded in the dorsal root of the lateral line nerves that carries only electrosensory fibers (New and Bodznick, 1985). High impedance (>20 MΩ) glass pipettes were necessary to isolate single units in the nerve. Recordings in the DON were made using tungsten electrodes (5–20 MΩ). Although multi-unit activity (hash) was audible in the superficial layer of the DON during stimulation, single

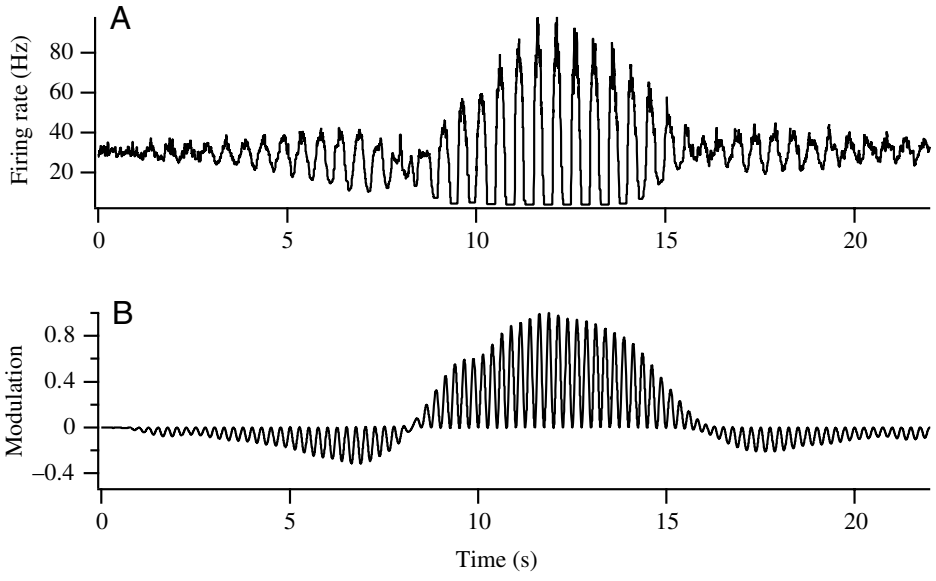

Fig. 1. Responses of a DON neuron to a 2 Hz sinuosidal electric field moved at 0.5 cm s^{-1} along the rostro-caudal axis of the rostrum. (A) Firing rate as a function of time. (B) As in A, but filtered and multiplied by the 2 Hz stimulus, showing the phase relationship of the response to the stimulus.

units could be isolated easily in the intermediate layer of the DON. It is unlikely that these units were incoming afferent fibers because it was impossible to isolate single units in the nerves with these metal electrodes. Furthermore, electrodes in the DON could be moved over a range of up to 50 μm without losing the unit, whereas units in the nerve were easily lost even with the slightest touch of the manipulator.

Whilst it is safe to assume that we were recording from cells in the DON and not from PA fibers, we do not know from which cell types we were recording. At least one class of neurons have ascending projections to the midbrain (Hofmann et al., 2002), but it is not known how many other cell types are present in the DON of the paddlefish.

The physiological properties of the recorded units in the DON are so similar, however, that we conclude that the recordings were only from one cell type with large cell bodies. Below we describe the response properties of these cells and compare them with those of primary afferent fibers to characterize the processing of electrosensory signals in the DON.

Spontaneous activity

The spontaneous rates of 30 PA fibers were measured, and range from 10 to 75 Hz with a mean rate of 44.22±14.73 Hz. From the spike data, the instantaneous frequency plot was computed and the average root mean square calculated (8.05±3.60 Hz), reflecting the variability of PA interspike intervals. Spontaneous rates of DON units were lower (30.94±10.56 Hz, N=55, P<0.0001). The average root mean square (3.86±1.69 Hz) was significantly lower than in PA fibers (P<0.0001), indicating that the variability in interspike intervals was lower in DON units than in PA fibers.

Differences in the sequence of interspike intervals between DON units and PA fibers were detected by autocorrelation of the spike trains. Fig. 2 shows the autocorrelation of a PA fiber (A) and a DON unit (B). In the PA fibers, long range autocorrelation is clearly visible, but DON units show only some short-range autocorrelation. Fig. 2C shows autocorrelation values for 60 DON units and 31 PA fibers plotted against their mean firing rate. Most PA fibers show high autocorrelation values (6.10±5.05), but some are in the range of DON units (2.03±0.59). In contrast, DON units never show the high autocorrelation values observed in most PA fibers.

Sensitivity and frequency tuning

Frequency tuning and sensitivity was tested with uniform field, constant amplitude sine wave stimuli with frequencies between 0.05 and 20 Hz. A stimulus intensity (25 μV cm^{-1}) was chosen that avoided saturation of the firing rate (rates were <100 Hz, but cells can be driven up to 200–300 Hz). Fig. 3 shows the peak firing rates of PA fibers and DON cells during stimulation at different frequencies. There is no difference in frequency tuning between PA and DON units. Although we did not test for threshold at each frequency, our constant amplitude stimuli provided an estimate about the sensitivity of the units. However, no differences in sensitivity between PA and DON units could be observed with our fixed 25 μV cm^{-1} amplitude.

Receptive field size

A slowly moving sinusoidally modulated (2 Hz) stimulus was used to determine the location and spatial structure of the receptive fields of DON and PA units. The stimulus source was a small (4 mm) dipole oriented perpendicular to the rostrum (monopolar configuration). Fig. 4 shows the phase plots of the responses of 15 PA and 15 DON units. In both cases, the

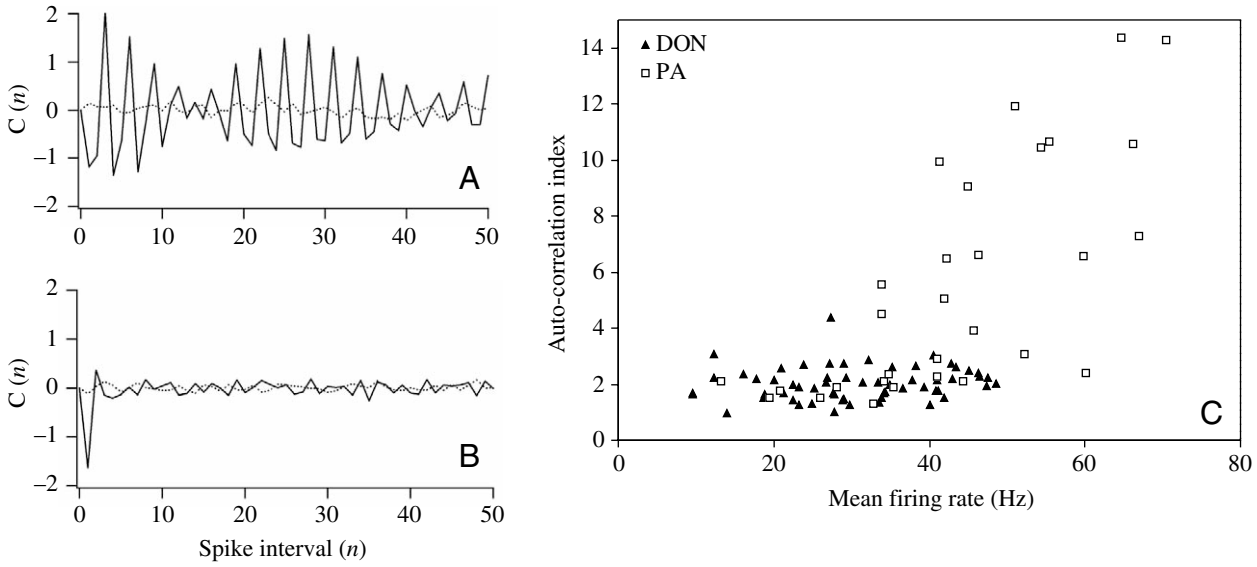

Fig. 2. Autocorrelation [C(n)] analysis of a primary afferent (PA) fiber (A) and a dorsal octavolateral nucleus (DON) unit (B). Solid lines, original data; dotted lines, shuffled data. Only the PA shows long-range autocorrelation. (C) Autocorrelation index of 30 PA fibers and 60 DON units plotted against the mean firing rate. Note the lack of higher autocorrelation values in DON units.

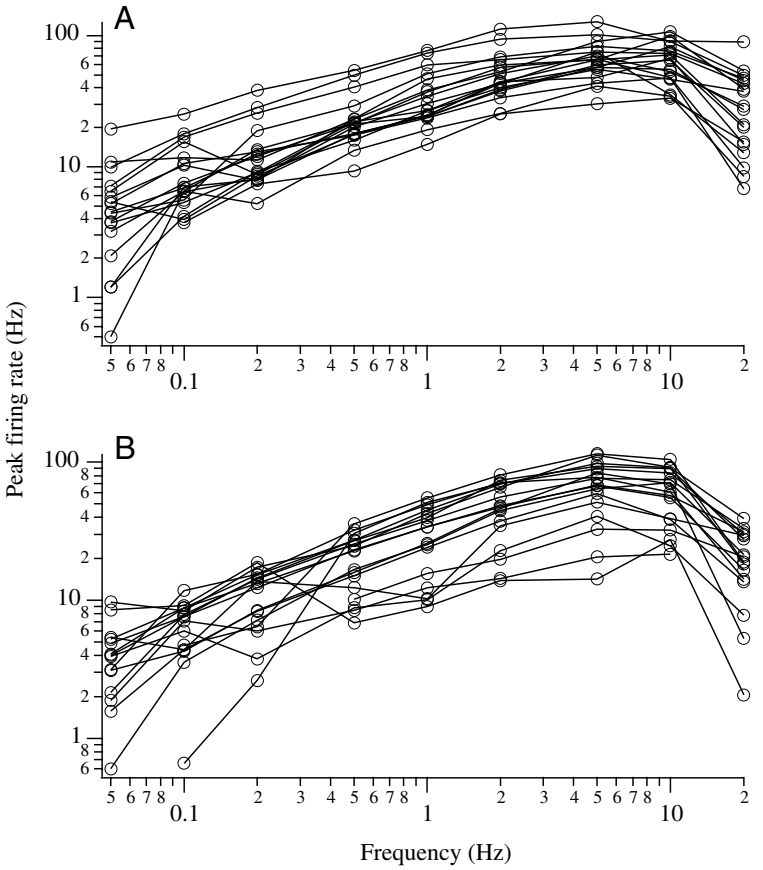

Fig. 3. Peak firing rate of primary afferent (PA) fibers (A) and dorsal octavolateral nucleus (DON) units (B) during stimulation with sinusoidal electric fields of different frequency. The response magnitudes at each stimulus frequency are similar and the overall frequency tuning curves are not different between PA fibers and DON units.

maximum response is reached when the electrode is at the center of the receptive field. In many cases, the positive peak is flanked by negative (phase inverted) responses. This is particularly pronounced in DON units. However, the negative response preceding the positive one is missing in units with receptive fields at the tip of the rostrum. Apparently, the negative response occurs only when the electrodes are over the rostrum, but not yet over the receptive field. Similar negative responses, but less pronounced, are also present in PA fibers.

The positive peak width (representing the size of the receptive field) is larger in DON units compared to PAs. Peak width was measured as the width at half maximum amplitude (2.11±0.4 s for PA fibers and 2.93±0.89 s for DON units, $P<0.05$).

Movement detection

In this set of experiments, we tested the responses of PA and DON neurons to an unmodulated DC stimulus with a moving dipole. The source dipole field was oriented perpendicular to the movement direction (monopolar configuration) and moved at a speed of 5 cm s^{-1}, which is equivalent to the normal swimming speed of the fish. Fig. 5 shows the change in firing rate of PA and DON units to the moving DC field, with traces aligned to the receptive field of the unit. The bottom trace in each panel is the average of the traces above. Both PA and DON units show very similar responses to the stimulus. DON responses showed a somewhat broader peak than those of PA fibers, as has been noted for the receptive field size (see above), although there is no evidence for differences in sensitivity to the moving stimulus.

Topography within the DON

In order to test for a topographic relationship between the location of the receptive fields on the skin surface and the location of the corresponding unit within the DON, we scanned the receptive field along the rostro-caudal axis as described in Materials and methods and plotted it relative to the location of the unit in the DON. Fig. 6A shows the location of receptive fields as a function of the location of the unit in the rostro-caudal axis of the DON. From the position of the unit within the DON, the location of the receptive field cannot be predicted. The same is true if the receptive field position is plotted against the location of the unit in the medio-lateral axis of the

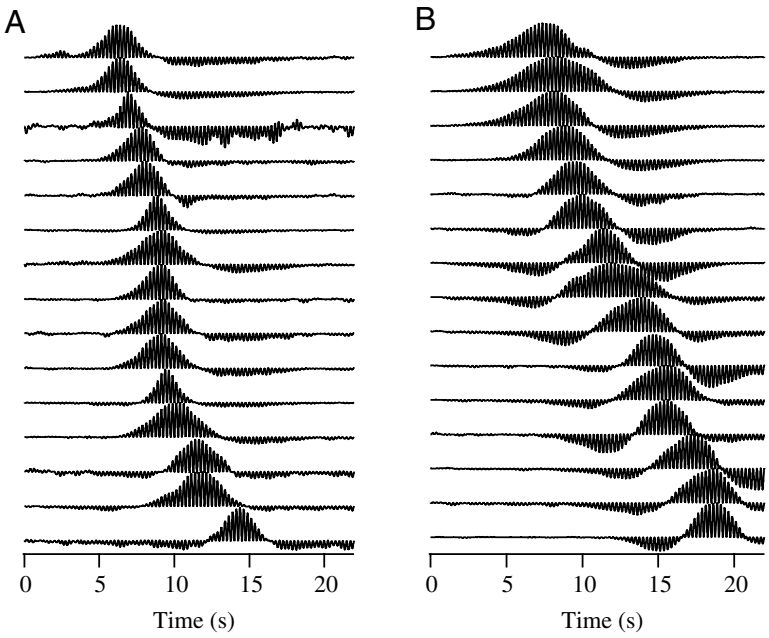

Fig. 4. Phase plots of the responses of 15 primary afferent (PA) fibers (A) and 15 dorsal octavolateral nucleus (DON) units (B) during stimulation with a small dipole field moved slowly along the rostro-caudal axis of the rostrum. Traces are sorted by the location of the receptive field. Stimulus frequency was 2 Hz and the speed 0.5 cm s^{-1}. Stimulus electrodes were oriented perpendicular to movement direction.

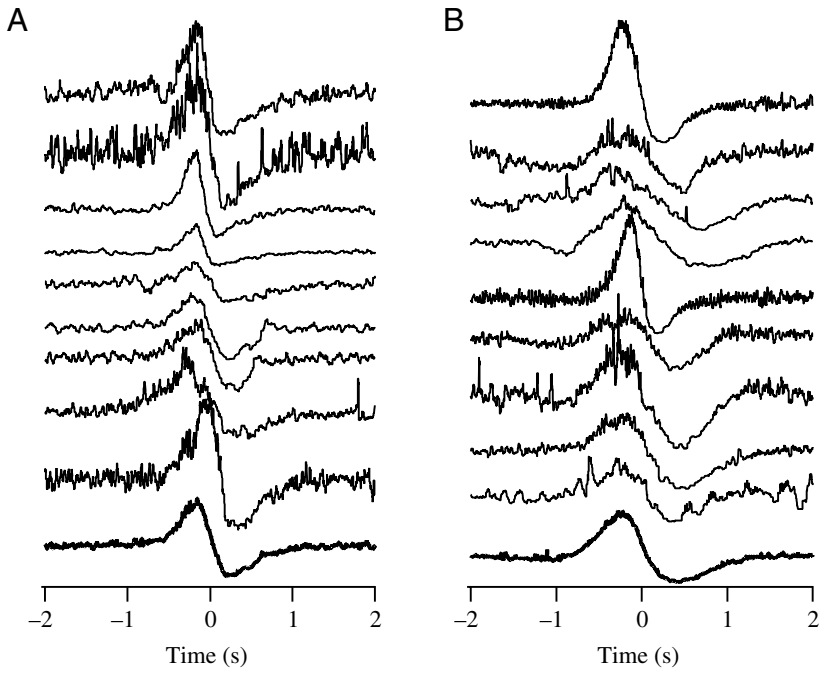

Fig. 5. Firing rates as a function of time for nine primary afferent (PA) fibers (A) and nine dorsal octavolateral nucleus (DON) units (B) during stimulation with a moving DC field (top nine traces); the lowest trace in each panel is the average. Traces are aligned by the receptive field position to allow averaging. The *x*-axis zero point marks the center of the receptive field. The speed of the DC stimulus was 5 cm s^{-1}. Response amplitude and shape were similar for PA fibers and DON units.

DON (Fig. 6B). The lack of any topography was also obvious during the recording session. For example, after recording a unit with a receptive field at the tip of the rostrum, a small advance of the electrode was equally likely to encounter a unit with its receptive field far away, e.g. at the gill cover. For receptive fields on the rostrum, we also noted whether the unit was on top of the rostrum or on the ventral surface. Again, there was no correlation with either the rostro-caudal or medio-lateral position of the unit in the DON.

Discussion

Our comparison of the response properties in PA and DON units revealed few differences between them. It is important to note that we did not record from afferent fibers within the DON. PA fibers do innervate the dorsal part of the DON and it is possible that our DON recordings contain some afferent fiber activity, although we think this is unlikely for several reasons. In DON recordings, we used commercial tungsten electrodes with 2–20 MΩ impedance. Units in the DON could be readily encountered with

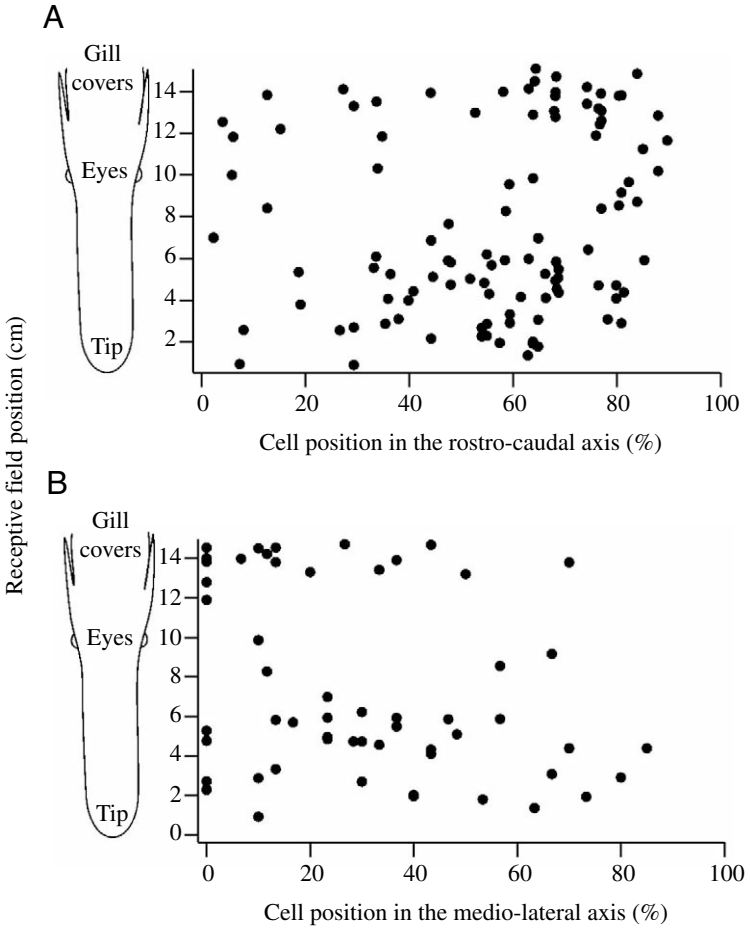

Fig. 6. *x–y* plots of receptive field position of dorsal octavolateral nucleus (DON) units *vs* cell location within the DON. The *y*-axis represents the normalized receptive field position. Zero is at the tip of the rostrum and 10 cm is the position of the nose opening just in front of the eye. Receptive field values for different sized fish were normalized and projected onto a standard fish with a tip-to-nose distance of 10 cm. (A) The *x*-axis represents the position of the cell along the rostro-caudal axis as % of total DON length. Zero represents the rostral end of the DON, 100 represents the caudal end of the DON. (B) The *x*-axis gives the cell position along the medio-lateral extent of the DON in percent. Zero means the medial border of the DON, 100 its lateral edge. Each symbol represents a DON unit whose receptive field position was measured. There is no correlation between the location of a cell in the DON and its receptive field along the rostro-caudal axis of the rostrum.

these electrodes in the DON and cells could be held for many hours, if desired. Furthermore, electrodes could be moved frequently over a distance up to 50 μm without losing the unit. In contrast, PA fibers in the nerve could never be isolated with the electrodes used in the DON. We were able to record multiunit 'hash' in the nerve and, in some cases, were able to hear individual units, but their spike amplitude was never sufficient to discriminate them from background activity as single units. To isolate single units in the nerve, we had to use glass pipettes with impedances of at least 30 MΩ. Even with these electrodes, units were not stable for very long, and any slight movement of the electrodes with the manipulator resulted in the loss of the unit.

Another reason why we are convinced that our DON recordings do not include PA fiber activity is that we did find differences between PA and DON units in their spontaneous activity. The firing rate is lower and more regular in DON neurons. Furthermore, autocorrelation analysis of DON and PA units shows that 61% of PA units have long-range autocorrelation values of more than 3 (see Fig. 2). From the 60 DON units analyzed, only one has an autocorrelation value higher than 3. Thus, based on the autocorrelation analysis, it is not likely that we were recording from afferent fibers in the DON. Long-range autocorrelations were described by Bahar et al. (2001) in the paddlefish electrosensory afferents, but our data show here, for the first time, that they are absent in secondary brain stem neurons. Although it is not clear what causes these autocorrelations, preliminary experiments show that they could be the result of the presence of multiple spike-generating zones in the afferent fiber. Two coupled oscillators with slightly different frequencies will cause alternating interspike intervals. In the autocorrelation analysis, this shows up as alternating positive and negative correlations since a long interval is followed by a short one and *vice versa*. The node or dip in the autocorrelation (Fig. 2A) may be caused by the interference of two different oscillation frequencies. This is similar to the beat frequency that exists if two oscillators with different frequencies are mixed. The frequency of this 'beating' represents the difference in frequencies of the two oscillators. In the periphery, branching of fibers into several myelinated roots has been described in the paddlefish (Wilkens and Hofmann, 2002) as well as in catfish (Peters and van Ieperen, 1989; Peters et al., 1997) and could indicate the presence of multiple oscillators. Whereas the mechanisms causing correlations in spike trains are not known, the functional significance may be in the suppression of low frequency noise (Chacron et al., 2004, 2005).

Comparison of paddlefish PA and DON activity with elasmobranchs shows that paddlefish neurons have a higher rate of spontaneous activity. In *Platyrhinoidis triseriata* and *Raja erinacea*, mean rates of PA are 8–18 Hz (New, 1990; Bodznick et al., 2003). Only *Raja eglanteria* shows PA rates as high as 45 Hz (Sisneros et al., 1998) that are similar to the 44 Hz found in the paddlefish. Spontaneous rates in sturgeons are 20–60 Hz (Teeter et al., 1980) and in catfish 50–100 Hz (Finger, 1986), values comparable to or exceeding the ones in the paddlefish. Finally, amphibian rates are 15 Hz (Münz et al., 1984; Schlegel and Roth, 1997) in the range of some elasmobranchs. Spontaneous rates for DON units are always lower than for PA fibers [e.g. 1.2 Hz in elasmobranchs (New, 1990) and 6 Hz in catfish (McCreery, 1977)]. The 31 Hz recorded here in the paddlefish DON are the highest found in any passive electrosensory animal. Also unique for the paddlefish is that DON units are more regular in their interspike intervals than PA fibers. In other animals, DON units are always described as being more irregular than PA fibers (McCreery, 1977; New, 1990; Bodznick et al., 2003).

There are also some differences in the paddlefish between PA and DON units that are revealed by slowly scanning their receptive fields. The size of the receptive field of DON units is slightly larger and the inhibitory surround is more pronounced than in PA fibers. In particular, the inhibitory surround resembles the receptive field organization in the visual system, where lateral inhibition mediated by retinal intermediates is responsible for the surround inhibition. However, we find inhibition in the paddlefish electrosensory system is already in PA fibers. Since there are no efferents from the brain innervating the receptors, PA fibers act completely independent of each other and it is not easy to understand how lateral inhibition could arise in the periphery. However, there is one possible explanation that does not require lateral inhibition at the neuronal level. While approaching the receptive field with a stimulus electrode, the signal could take one of two paths to the receptor: one directly through the water to the pore of the receptor and the other through the skin next to the stimulus electrode and through the animal to the base of the receptor cells. This latter path would reverse the effect on the receptor, since it is basically stimulating the internal reference of the receptor. If the internal tissue resistance is much lower than the water resistance, this path could have an overall resistance lower than the path through the water and therefore dominate the response if the stimulus electrodes are far from the receptive field, but close to another skin area. To test this hypothesis, a detailed study of skin and tissue impedances is required.

Apart from this slight difference, we were struck by the overall similarities of PA and DON responses and the question arises what function can be attributed to the DON in signal processing. In a previous paper (Hofmann et al., 2004) on temporal information processing in the paddlefish electrosensory system, we showed that the DON cells compute the first derivative in time of the electric fields at the receptor. One property defining the first derivative is that the gain is proportional to the frequency. This results in a linear slope of the frequency tuning curve that has been found in virtually all passive electrosensory animals (Bretschneider et al., 1985; Peters and Evers, 1985; Kalmijn, 1988; Andrianov et al., 1996; Schlegel and Roth, 1997; Tricas and New, 1998; Bodznick et al., 2003). A large part of the processing toward the first derivative, however, could be attributed to the PA or receptor cells, since the frequency tuning curve of the PA already shows a relatively good linear relationship between gain and

frequency (Fig. 3). Perhaps the most important function of the DON that has yet to be investigated in the paddlefish is the cancellation of noise. An animal's own movements cause modulations in the discharge rate of electroreceptors that are canceled out by common mode rejection and adaptive filters, as found mainly in elasmobranchs (Montgomery, 1984; Montgomery and Bodznick, 1999; Bodznick et al., 2003). Adaptive filters involve massive descending input from the cerebellum into a part of the DON termed the crista cerebellaris. Since this structure is well developed in the paddlefish, adaptive filter mechanisms are probably employed in the paddlefish DON as well.

The most surprising result of our investigation is the lack of a topographic relationship between receptive fields in the skin and the position of the corresponding neurons in the DON. Although we have not looked for topography in the dorso-ventral axis (depth), we think topography in this axis is unlikely since the DON is organized in layers, with the PA fibers entering dorsally. Principle efferent neurons are located below in a thinner horizontal layer (Hofmann et al., 2002). In other layered structures like the cortex or midbrain tectum, topography is always organized perpendicular to the layers. In the DON of the little skate, Bodznick and Schmidt (1984) reported some topographical order when the electrode was advanced dorso-ventrally, but in this animal the DON is oriented obliquely and their figures clearly show that the apparent dorso-ventral topography is in fact a medio-lateral one. There is no evidence for a topography across the different layers of the DON.

In many sensory systems, information from arrays of receptors is processed in topographic maps. This is particularly important in modalities that reveal information about the location of objects in space. The paddlefish electrosensory system apparently breaks that rule. Behavioral studies have clearly shown that the electrosensory system alone is sufficient to localize objects in space (Wilkens et al., 2001), yet there is no topographic map in the brain stem. This is even more puzzling since topographic maps were found in other passive electrosensory animals (Bodznick and Schmidt, 1984; New and Singh, 1994). However, these studies only examined PA projections, either by tracers applied to different branches of the lateral line nerves to study their termination zones or by multiunit activity recorded within the superficial fiber layer of the DON. There is no comparable study on the location of second order cells within the DON in relation to their receptive fields. More detailed studies are needed to solve this problem, but two lines of thought may be considered.

Topographic organization in the central nervous system could be for two reasons. First, it could have a true function. An orderly arrangement of receptive fields in a topographic map may be required for lateral computations such as contrast enhancement or movement detection. For these spatial computations, a neuron that sends collaterals to neighboring neurons has to rely on the fact that the neighboring neurons also have adjacent receptive fields in the periphery. Second, topography could be the consequence of developmental constraints, without serving any physiological function. Preliminary tracer studies in the paddlefish showed that the primary projections from the lateral line nerve innervating the rostrum and a branch innervating the electroreceptors on the gill cover form separate terminal fields in the DON, with the rostrum nerve terminating more laterally than the gill cover branch. This confirms earlier studies in catfish and elasmobranchs (Bodznick and Schmidt, 1984; New and Singh, 1994). However, our data on second order DON cells showed that this projection pattern does not lead to a topographic distribution of cells in the DON. This suggests that the projection pattern of the different branches of the lateral line nerves within the DON may be due to the fact that fibers from different branches tend to stay together and not intermingle with each other. The developmental sequence of invading pioneer fibers of the lateral line nerves may determine a coarse 'topography' that does not necessarily serve any physiological function.

Another misconception is that a topographic map is required to preserve topographic information. As mentioned above, a topographic map may be required for spatial information processing between neighboring receptor channels. In the paddlefish, we found little sign of spatial information processing within the DON, such as contrast enhancement or movement detection, and no topographic organization. Yet, DON neurons show well-defined receptive fields, and behavioral studies clearly showed that paddlefish use spatial information about prey location for feeding (Wilkens et al., 2001). However, if we look closely at the coordinate systems involved, we find that the distance of the source from the detecting fish is an important factor in determining the behavioral response. This dimension is not present in a simple somatotopic body map and has to be extracted computationally. An important sensori-motor interface mediating prey capture is the mesencephalic tectum (TM), and it has been shown that major ascending electrosensory pathways reach this structure (Hofmann et al., 2002). Although not yet investigated in the paddlefish, the TM is topographically organized in all vertebrates investigated so far. This has been shown mainly for the visual system that projects to the TM in all vertebrates. An object in front of the animal would be represented in a frontal field of the TM and an object more lateral would be represented in a different location, i.e. more laterally. If we assume that this is also the case in the paddlefish and if we further assume that electrosensory information reaching the TM carries topographic information that is in register with the visual world, an object at the tip of the rostrum of the paddlefish would be represented in the frontal field and an object centered at the same 'somatotopic' location, but further from the skin surface, would be represented more laterally. In other words, an object centered at the same 'somatotopic' location, but at different distances, would be represented in different locations in the TM. A somatotopic map in the DON simply to preserve spatial information is thus not a satisfactory explanation since the somatotopic map would have to be transformed anyway into a

spherical map that contains distance information, at least for skin locations remote from the eye.

But how can an array of receptors compute the distance to the source? Initial calculations by Kalmijn (1988) and a more detailed analysis (Hofmann and Wilkens, 2005), showed that there is sufficient information in the time domain in each receptor channel. A single receptor traversing an electric field receives an electrical signal over time that contains sufficient information necessary to extract the location, including the distance, of the source, independent of source amplitude, size and orientation. The computation algorithm involves an analysis in the time domain, but does not require a spatial analysis. It is intriguing that an important step in this algorithm is the computation of the first derivative, which matches very well the behavior of DON units (Hofmann et al., 2004).

We still have to show that the paddlefish, and perhaps other electrosensory animals, actually compute the temporal structure of electrical events rather than, or in addition to, the spatial structure still useful at short distances. What we have shown so far, however, is that the initial step in signal processing in the DON is perfectly suited to preserve temporal information (Hofmann et al., 2004) and, in this study, that there is no topographic map of the body surface within the DON and little sign of spatial information processing such as lateral inhibition, contrast enhancement or movement detection, at least at the level of the brain stem.

This research was supported by grants from the DFG (HO 1602/3-1), NSF/DAAD, the National Science Foundation (IOB-0524869), and a University of Missouri Research Board grant. The experiments comply with the 'Principles of animal care', publication No. 86-23, revised 1985, of the National Institute of Health and with the current Missouri State laws.

References

Andrianov, G. N., Bretschneider, F. and Peters, R. C. (1996). Mode of operation of ampullary electroreceptor organs of freshwater catfish. *Prim. Sensory Neuron* **1**, 231-242.

Bahar, S., Kantelhardt, J. W., Neimann, A., Rego, H. H. A., Russell, D. F., Wilkens, L., Bunde, A. and Moss, F. (2001). Long-range temporal anti-correlations in paddlefish electroreceptors. *Europhys. Lett* **56**, 454-460.

Bodznick, D. and Boord, R. L. (1986). Electroreception in chondrichthyes. Central anatomy and physiology. In *Electroreception* (ed. T. H. Bullock and W. Heiligenberg), pp. 225-256. New York: John Wiley & Sons.

Bodznick, D. and Northcutt, R. G. (1981). Electroreception in lampreys: evidence that the earliest vertebrates were electroreceptive. *Science* **221**, 465-467.

Bodznick, D. and Schmidt, A. (1984). Somatotopy within the medullary electrosensory nucleus of the little skate, *Raja erinacea*. *J. Comp. Neurol.* **225**, 581-590.

Bodznick, D., Montgomery, J. and Tricas, T. C. (2003). Electroreception: extracting behaviorally important signals from noise. In *Sensory Processing in Aquatic Environments* (ed. S. P. Collin and N. J. Marshall), pp. 389-403. Berlin: Springer.

Bretschneider, F., De Weille, J. R. and Kilis, J. F. L. (1985). Functioning of catfish electroreceptors: fractional-order filtering and non-linearity. *Comp. Biochem. Physiol.* **80A**, 191-198.

Chacron, M. J., Lindner, B. and Longtin, A. (2004). Noise shaping by interval correlations increases information transfer. *Physical Rev. Lett.* **92**, 080601.

Chacron, M. J., Maler, L. and Bastian, J. (2005). Electroreceptor neuron dynamics shape information transmission. *Nature Neurosci*. **8**, 673-678.

Finger, T. E. (1986). Electroreception in catfish. Behavior, anatomy, and electrophysiology. In *Electroreception* (ed. T. H. Bullock and W. Heiligenberg), pp. 465-482. New York: John Wiley & Sons.

Finger, T. E., Bell, C. C. and Carr, C. E. (1986). Comparisons among electroreceptive teleosts: why are electrosensory systems so similar? In *Electroreception* (ed. T. H. Bullock and W. Heiligenberg), pp. 465-482. New York: John Wiley & Sons.

Fortune, E. S. and Rose, G. J. (1997). Temporal filtering properties of ampullary electrosensory neurons in the torus semicircularis of *Eigenmannia*: evolutionary and computational implications. *Brain Behav. Evol.* **49**, 312-323.

Fritzsch, B. and Münz, H. (1986). Electroreception in amphibians. In *Electroreception* (ed. T. H. Bullock and W. Heiligenberg), pp. 483-496. New York: John Wiley & Sons.

Gregory, J. E., Iggo, A., McIntyre, A. K. and Proske, U. (1987). Electroreceptors in platypus. *Nature* **326**, 386-387.

Gurgens, C., Russell, D. F. and Wilkens, L. A. (2000). Electrosensory avoidance of metal obstacles by the paddlefish. *J. Fish. Biol.* **57**, 277-290.

Hofmann, M. H. and Wilkens, L. A. (2005). Temporal analysis of moving dc electric fields in aquatic media *Phys. Biol.* **2**, 23-28.

Hofmann, M. H., Wojtenek, W. and Wilkens, L. A. (2002). Central organization of the electrosensory system in the paddlefish (*Polyodon spathula*). *J. Comp. Neurol.* **446**, 25-36.

Hofmann, M. H., Falk, M. and Wilkens, L. A. (2004). Electrosensory brain stem neurons compute the time derivative of electric fields in the paddlefish. *Fluct. Noise Lett*. **4**, L129-L138.

Kalmijn, A. J. (1966). Electro-perception in sharks and rays. *Nature* **212**, 1232-1233.

Kalmijn, A. J. (1984). Theory of electromagnetic orientation: a further analysis. In *Comparative Physiology of Sensory Systems* (ed. L. Bolis, R. D. Keynes and S. H. P. Maddrell), pp. 525-560. Cambridge: Cambridge University Press.

Kalmijn, A. J. (1988). Detection of weak electric fields. In *Sensory Biology of Aquatic Animals* (ed. J. Atema), pp. 151-186. New York: Springer.

McCreery, D. B. (1977). Two types of electroreceptive lateral lemniscal neurons of the lateral line lobe of the catfish *Ictalurus nebulosus*: connections from the lateral line nerve and steady-state frequency response characteristics. *J. Comp. Physiol*. **113**, 317-339.

Montgomery, J. C. (1984). Frequency response characteristics of primary and secondary neurons in the electrosensory system of the thornback ray. *Comp. Biochem. Physiol.* **79A**, 189-195.

Montgomery, J. C. and Bodznick, D. (1999). Signals and noise in the elasmobranch electrosensory system. *J. Exp. Biol.* **202**, 1349-1355.

Münz, H., Claas, B. and Fritzsch, B. (1984). Electroreceptive and mechanoreceptive units in the lateral line of the axolotl *Ambystoma mexicanum. J. Comp. Physiol. A* **154**, 33-44.

New, J. G. (1990). Medullary electrosensory processing in the little skate. I. Response characteristics of neurons in the dorsal octavolateralis nucleus. *J. Comp. Physiol. A* **167**, 285-294.

New, J. G. and Bodznick, D. (1985). Segregation of electroreceptive and mechanoreceptive lateral line afferents in the hindbrain of chondrostean fishes. *Brain Res.* **336**, 89-98.

New, J. G. and Singh, S. (1994). Central topography of anterior lateral line nerve projections in the channel catfish, *Ictalurus punctatus*. *Brain Behav. Evol*. **43**, 34-50.

Northcutt, R. G. (1986). Electroreception in nonteleost bony fishes. In *Electroreception* (ed. T. H. Bullock and W. Heiligenberg), pp. 257-285. NewYork: John Wiley & Sons.

Peters, R. C. and Evers, H. P. (1985). Frequency selectivity in the ampullary system of an elasmobranch fish (*Scyliorhinus canicula*). *J. Exp. Biol.* **118**, 99-109.

Peters, R. C. and van Ieperen, S. (1989). Resting discharge and sensitivity of ampullary electroreceptors in *Clarias gariepinus* related to convergence ratio during ontogeny. *Brain Behav. Evol.* **34**, 43-47.

Peters, R. C., Brans, R. J., Bretschneider, F., Versteeg, E. and Went, A. (1997). Converging electroreceptor cells improve sensitivity and tuning. *Neurosci.* **81**, 297-301.

Pettigrew, J. D. (1999). Electroreception in monotremes. *J. Exp. Biol.* **202**, 1447-1454.

Roth, A. (1973). Electroreceptors in Brachiopterygii and Dipnoi. *Naturwissenschaften* **60**, 106.

Roth, A. and Schlegel, P. (1988). Behavioral evidence and supporting

electrophysiological observations for electroreception in the blind cave salamander *Proteus anguinus*, urodela. *Brain Behav. Evol.* **32**, 277-280.

Schlegel, P. A. and Roth, A. (1997). Tuning of electroreceptors in the blind cave salamander, *Proteus anguinus* L. *Brain Behav. Evol.* **49**, 132-136.

Sisneros, J. A., Tricas, T. C. and Luer, C. A. (1998). Response properties and biological function of the skate electrosensory system during ontogeny. *J. Comp. Physiol. A.* **183**, 87-99.

Teeter, J. H., Szamier, R. B. and Bennett, M. V. L. (1980). Ampullary electroreceptors in the sturgeon *Scaphirhynchus platorynchus* (Rafinesque). *J. Comp. Physiol.* **138**, 213-223.

Tricas, T. C. and New, J. G. (1998). Sensitivity and response dynamics of elasmobranch electrosensory primary afferent neurons to near threshold fields. *J. Comp. Physiol. A* **182**, 89-101.

Wilkens, L. A. and Hofmann, M. H. (2002). The electric sense of the paddlefish: a passive system for the detection and capture of zooplankton prey. *J. Physiol. (Paris)* **96**, 363-377.

Wilkens, L. A. and Hofmann, M. H. (2004). The behavior of animals with a low-frequency, passive electrosensory system. In *Electroreception* (ed. T. H. Bullock, C. D. Hopkins, A. N. Popper and R. R. Fay), pp. 229-263. New York: Springer.

Wilkens, L. A., Wettring, B., Wagner, E., Wojtenek, W. and Russell, D. F. (2001). Prey detection in selective plankton feeding by the paddlefish: is the electric sense sufficient? *J. Exp. Biol.* **204**, 1381-1389.